J. Korean Soc. Ind. Appl. Math. Vol.24, No.2, 215–227, 2020 http://doi.org/10.12941/jksiam.2020.24.215

A LOCAL CONSERVATIVE MULTISCALE METHOD FOR ELLIPTIC PROBLEMS WITH OSCILLATING COEFFICIENTS

YOUNGMOK JEON[1] AND EUN-JAE PARK[2†]

[1]DEPARTMENT OF MATHEMATICS, AJOU UNIVERSITY, SUWON, 16499, REPUBLIC OF KOREA.

[2]DEPARTMENT OF COMPUTATIONAL SCIENCE AND ENGINEERING, YONSEI UNIVERSITY, SEOUL, 03722, REPUBLIC OF KOREA.

Email address: †ejpark@yonsei.ac.kr.

ABSTRACT. A new multiscale finite element method for elliptic problems with highly oscillating coefficients are introduced. A hybridization yields a locally flux-conserving numerical scheme for multiscale problems. Our approach naturally induces a homogenized equation which facilitates error analysis. Complete convergence analysis is given and numerical examples are presented to validate our analysis.

1. INTRODUCTION

In this paper we consider the following elliptic problem:

$$\begin{aligned} L_\epsilon(u_\epsilon) = -\nabla \cdot (a_\epsilon \nabla u_\epsilon) &= f \quad \text{on } \Omega, \\ u_\epsilon &= 0 \quad \text{on } \partial\Omega. \end{aligned} \tag{1.1}$$

Here, and in what follows, we assume $a_\epsilon(x) = a(y)$ for a 1-periodic, positive definite and symmetric tensor a and $y = \frac{x}{\epsilon}$. The domain Ω is a convex polygonal domain.

Many problems in material science, chemistry, fluid dynamics and biology are governed by multiscale problems with highly oscillatory coefficients [1, 2, 3, 4]. For example, the properties of a composite material or the heterogeneity of porous media has oscillatory nature. It is well known that standard finite element methods do not yield good numerical approximations for such problems with rapidly oscillating coefficients when the mesh size is $h > \epsilon$. To obtain computationally feasible system, multiscale approach is essential for (1.1). For example, the multiscale finite element methods (MsFEM) [5, 6, 7, 8] use oversampling to construct basis functions adapted to oscillation in solutions. Variational multiscale methods (VMS) [3] or the residual-free bubble function methods (RFB) [9, 10] use enhanced trial/test spaces to resolve fine scale nature of the problem. The heterogeneous multiscale method (HMM) is a methodology for designing sublinear scaling algorithms by exploiting scale separation and the other features of the problem [11, 12]. The generalized FEM for homogenization problems is proposed in [13]. The multiscale domain decomposition approach can be found in [14, 15, 16, 17], where the flux continuity is imposed via a mortar finite element space on a coarse grid scale, while the equations in the coarse elements (or subdomains) are discretized on a fine grid scale.

The numerical method proposed in this paper is related to cell boundary element methods (CBE) [18, 19, 20, 21, 22] and hybridization [23, 24, 25, 26]. The CBE method can be interpreted as a finite

Received by the editors June 5 2020; Accepted June 16 2020; Published online June 25 2020.

2010 *Mathematics Subject Classification.* 65N30, 35B27, 74Q15.

Key words and phrases. cell boundary element, homogenization, variational multiscale, multiscale finite element, hybridization, mass conservation.

† Corresponding author.

element version of the finite volume method (FVM). The CBE method is defined on the finite element mesh and preserves flux in each local cell. Moreover, global flux conservation holds for a class of CBE methods. The flux preserving property of numerical methods is very desirable for transport problems. For example in underground flow problems it is shown that the multiscale finite volume method, which is a flux preserving method, produces well approximating numerical solutions [27]. See also [1, 5, 23] for locally conservative multiscale methods based on the mixed finite element and discontinuous Galerkin method.

In this paper, we introduce a new multiscale method based on a hybridization of flux-continuity across cell interfaces. From here on we call it as locally conservative multiscale finite element (LC-MsFE) method. The LC-MsFE method is a multiscale realization of the cell boundary element methods. More precisely, the method is composed of the following processes. Suppose K is any triangle of a triangulation $\mathcal{T}_h$ and $\mathcal{K}_h$ is the *skeleton* of $\mathcal{T}_h$ (see (3.1)).

: Step 1. Set $u_\epsilon = v_\epsilon + g_f$, where v_ϵ and g_f are solutions of elliptic equations:

$$-\nabla \cdot (a_\epsilon \nabla v_\epsilon) = 0 \text{ in } K, \qquad v_\epsilon = \lambda_\epsilon \text{ on } \partial K, \tag{1.2}$$

$$-\nabla \cdot (a_\epsilon \nabla g_f) = f \text{ in } K, \qquad g_f = 0 \text{ on } \partial K \tag{1.3}$$

with $\lambda_\epsilon = u_\epsilon|_{\mathcal{K}_h}$.

: Step 2. Use jump of normal flux at cell interfaces being zero,

$$[[a_\epsilon \nabla v_\epsilon]] = -[[a_\epsilon \nabla g_f]] \quad \text{on each edge } e \subset \mathcal{K}_h,$$

to obtain a global coarse system in unknowns λ_ϵ only.

The Eq. (1.2) can be solved by using the oversampling technique [7] to capture oscillatory boundary condition $v_\epsilon = \lambda_\epsilon$ on ∂K as in [18]. In the oversampling method the Eq. (1.2) is solved in an oversampling domain K', $K \subset K'$, for each basis of $P_1(\partial K') := P_1(K')|_{\partial K'}$ with a numerical solver. Then, restrictions of the solutions to K form a basis for approximation of v_ϵ which captures the oscillatory nature of solutions very well. However, the cost for solving (1.2) can be costly if the scale ratio, $\sqrt{|K'|}/\epsilon$, is very large. In this paper, to treat problems of a large scale ratio more efficiently, we take a variational multiscale approach in solution procedure for the Eq. (1.2). In the variational multiscale approach we further decompose v_ϵ as $v_\epsilon = v_0 + v_1$, where v_0 is a *coarse* scale solution and v_1 is a highly oscillatory part (*fine* scale resolution) of v_ϵ with vanishing average. Indeed, v_1 will be determined by v_0 and then v_ϵ is determined by v_0. Therefore, *Step 2* induces a square system with $v_0|_{\mathcal{K}_h}$ as only unknowns. Moreover, the Eq. (1.3) can be replaced in our new approach with a coarse scale solution: for example,

$$-\nabla \cdot (\overline{a} \nabla g_0) = \overline{f} \text{ in } K, \qquad \int_e g_0 ds = 0 \text{ on } e \subset \partial K,$$

where $\overline{a} = \frac{1}{|Y|}\int_Y a(y)dy$ and $Y = [0,1]^2$ with its volume $|Y|$. This will reduce computational cost additionally without losing accuracy of the method.

The rest of the paper is organized as follows. In §2 the homogenization theory in a periodic setting is reviewed. In §3 localization and solution decomposition are introduced. In §4 we introduce multiscale basis functions for the LC-MsFE method. Simple calculation yields that our method can be viewed as a finite element method for the homogenized equation. Also we note that the LC-MsFE method preserves flux locally. Optimal, resonance free convergence analysis is provided for the LC-MsFE method. In the last section we provide numerical experiments of our method. We consider two kinds of fine scale resolvers, the spectral and the oversampling approaches. Some computational issues such as ϵ-interference in error and phase-shift error are covered.

2. HOMOGENIZATION

In this section we review the well known homogenization theory [2, 28]. Consider a power series expansions:

$$\begin{aligned} u_\epsilon(x) &= u_0(x,y) + \epsilon u_1(x,y) + \epsilon^2 u_2(x,y) + \cdots \\ p_\epsilon(x) &= p_0(x,y) + \epsilon p_1(x,y) + \epsilon^2 p_2(x,y) + \cdots \end{aligned} \tag{2.1}$$

where $p_\epsilon = a_\epsilon \nabla u_\epsilon$ and $y = \frac{x}{\epsilon}$ from here on. From the relations, $p_\epsilon = a_\epsilon \nabla u_\epsilon$ and $-\nabla \cdot p_\epsilon = f$ one obtains

$$\begin{aligned} p_0 + \epsilon p_1 + \epsilon^2 p_2 \cdots &= a_\epsilon(\nabla_x u_0 + \frac{1}{\epsilon}\nabla_y u_0 + \epsilon \nabla_x u_1 + \nabla_y u_1 + \epsilon^2 \nabla_x u_2 + \cdots) \\ f &= -(\nabla_x \cdot p_0 + \frac{1}{\epsilon}\nabla_y \cdot p_0 + \epsilon \nabla_x \cdot p_1 + \nabla_y \cdot p_1 + \cdots) \end{aligned}$$

Collecting terms with the same power of ϵ from (2.1), one has

$$\begin{aligned} O(\epsilon^{-1}): &\qquad a_\epsilon \nabla_y u_0 = 0, \\ O(\epsilon^{-1}): &\qquad -\nabla_y \cdot p_0 = 0, \\ O(\epsilon^{0}): &\qquad a_\epsilon \nabla_y u_1 + a_\epsilon \nabla_x u_0 = p_0, \\ O(\epsilon^{0}): &\qquad -\nabla_y \cdot p_1 - \nabla_x \cdot p_0 = f \end{aligned}$$

and so on. Then the homogenized solution u_0 satisfies

$$\begin{aligned} L_0(u_0) = -\nabla \cdot (a_0 \nabla u_0) = f \qquad &\text{in } \Omega, \\ u_0 = 0 \qquad &\text{on } \partial\Omega, \end{aligned} \tag{2.2}$$

where

$$a_0 = \frac{1}{|Y|}\int_Y a(I + \nabla_y \chi) dy.$$

Here, $\chi = (\chi_1, \chi_2)$ is a periodic solution of

$$-\nabla_y \cdot (a(y)\nabla_y \chi) = \nabla_y \cdot a(y) \tag{2.3}$$

with $\int_Y \chi dy = \mathbf{0}$. Moreover, we have

$$u_1(x,y) = \chi(y)\nabla u_0(x).$$

From here and on, differential operators are applied column-wise so that $\nabla\chi := (\nabla\chi_1, \nabla\chi_2)$ for $\chi = (\chi_1, \chi_2)$ and $\nabla \cdot a := (\nabla \cdot a_1, \nabla \cdot a_2)$ for matrix a with column vectors a_1 and a_2.

Since $u_0(x) + \epsilon u_1(x,y) \neq u_\epsilon(x)$ on $\partial\Omega$, due to the periodicity of u_1, one can introduce a correction θ which satisfies

$$\begin{aligned} -\nabla \cdot a_\epsilon \nabla\theta = 0 \qquad &\text{in } \Omega, \\ \theta = -u_1 \qquad &\text{on } \partial\Omega. \end{aligned}$$

Summarizing the above results, we have an expansion of u_ϵ as follows:

$$u_\epsilon(x) = u_0(x) + \epsilon u_1(x,y) + \epsilon\theta(x,y) + r(x,y). \tag{2.4}$$

Moreover, the following estimates hold by the Calderon-Zygmund inequality and by results from [28] and [6]:

$$\begin{aligned} \|u_0\|_{2,\Omega} &\lesssim \|f\|_{0,\Omega}, \\ \|\epsilon\nabla\theta\|_{0,\Omega} &\lesssim \sqrt{\epsilon}(\|u_0\|_{2,\Omega} + \|u_0\|_{1,\infty,\Omega}), \\ \|r\|_{1,\Omega} &\lesssim \epsilon\|u_0\|_{2,\Omega} \end{aligned} \tag{2.5}$$

and

$$\|u_\epsilon - u_0\|_{0,\Omega} \lesssim \epsilon \|u_0\|_{2,\Omega}. \tag{2.6}$$

Here, $\|\cdot\|_{k,\Omega}$ denotes the usual Sobolev space norm and $A \lesssim B$ denotes $A \leq cB$ for some positive constant c, independent of h and ϵ.

3. Localization and solution decompositions

We begin with introducing some mathematical notations. The family $\mathcal{T}_h$ is shape-regular triangulation of Ω into triangles with $h = \max_{K\in\mathcal{T}_h} h_K$, where h_K denotes the diameter of $K \in \mathcal{T}_h$. Let $\mathcal{E}_h$ denote the set of edges e of the triangulation $\mathcal{T}_h$ and $\mathcal{V}_h$ the set of the midpoint of each edge. Therefore, for each $p \in \mathcal{V}_h$ there exists an associated edge $e_p \in \mathcal{E}_h$. We set the *skeleton* of the mesh $\mathcal{T}_h$ as

$$\mathcal{K}_h = \cup_{K\in\mathcal{T}_h} \partial K. \tag{3.1}$$

Now, let us introduce function spaces. The space $L_p(D)$ is the usual L_p space with the norm $\|\cdot\|_{L_p(D)}$ for $1 \leq p \leq \infty$. The space $W_p^s(D)$ is the standard Sobolev space with the norm $\|\cdot\|_{s,p,D}$ and its subspace $W_{p,0}^s(D)$ denotes the space of functions with vanishing traces. We employ the abbreviations $H^s(D)$ for $W_2^s(D)$, $H_0^s(D)$ for $W_{2,0}^s(D)$ with norms and seminorms $\|\cdot\|_{s,D}$ and $|\cdot|_{s,D}$ for $\|\cdot\|_{s,2,D}$ and $|\cdot|_{s,2,D}$, respectively.

In order to derive the multiscale FE method we consider the following localized problem: for each cell $K \in \mathcal{T}_h$,

$$\begin{aligned} -\nabla\cdot a_\epsilon \nabla u_\epsilon &= f \quad \text{in } K, \\ [[a_\epsilon \nabla u_\epsilon]] &= 0 \quad \text{on } e = \partial K \cap \partial K'. \end{aligned} \tag{3.2}$$

Here,

$$[[a_\epsilon \nabla u_\epsilon]] = (a_\epsilon \nabla u_\epsilon)\cdot \nu + (a_\epsilon \nabla u_\epsilon)\cdot \nu'$$

denotes jumps of normal fluxes across intercell boundaries. The continuity of normal fluxes in (3.2) can be weakened as follows:

$$\int_{\mathcal{K}_h} [[a_\epsilon \nabla u_\epsilon]] w ds = 0 \quad \text{for } w \in H_0^1(\Omega). \tag{3.3}$$

Consider a local solution decomposition:

$$u_\epsilon = v_\epsilon + g_f, \tag{3.4}$$

where v_ϵ and g_f satisfy

$$\begin{aligned} -\nabla\cdot a_\epsilon \nabla v_\epsilon &= 0 \qquad \text{in } K, \\ v_\epsilon &= u_\epsilon \qquad \text{on } \partial K \end{aligned} \tag{3.5}$$

and

$$\begin{aligned} -\nabla\cdot a_\epsilon \nabla g_f &= f \qquad \text{in } K, \\ g_f &= 0 \qquad \text{on } \partial K, \end{aligned} \tag{3.6}$$

respectively.

Invoking (3.3), v_ϵ and g_f satisfy

$$\int_{\mathcal{K}_h} [[a_\epsilon \nabla v_\epsilon]] w ds = -\int_{\mathcal{K}_h} [[a_\epsilon \nabla g_f]] w ds \quad \text{for } w \in H_0^1(\Omega).$$

This is the motivation of the hybridized finite element method. In the authors' previous work [18], the Eq. (3.5) is solved by a numerical method adopting the oversampling technique in [7]. The motivation of the oversampling technique is to catch the oscillating property of u_ϵ on ∂K.

We take a different approach, a variational multiscale technique. For this, we consider another solution decomposition for v_ϵ. As mentioned before, we find that we do not need an accurate approximation of g_f and this is another advantage of this method.

Let

$$v_\epsilon = v_0 + v_1, \tag{3.7}$$

where v_0 and v_1 satisfy

$$\begin{aligned} -\nabla\cdot(\overline{a}\nabla v_0) &= 0 \qquad \text{in } K, \\ v_0 &= u_0 \qquad \text{on } \partial K \end{aligned} \tag{3.8}$$

$$\begin{aligned} -\nabla\cdot(a_\epsilon\nabla v_1) = \nabla\cdot((a_\epsilon-\overline{a})\nabla v_0) &\qquad \text{in } K, \\ v_1 = u_\epsilon - u_0 &\qquad \text{on } \partial K, \end{aligned} \tag{3.9}$$

respectively. Here, $\overline{a} = \frac{1}{|Y|}\int_Y a(y)dy$, u_0 is a coarse scale homogenized solution so that $u_\epsilon - u_0$ ($\approx \epsilon\chi\nabla u_0$) is dominated by a periodic function with vanishing averages. The solution v_0 is called a *coarse scale* solution and v_1 is a *fine scale* resolution. In our numerical method the Eq. (3.8) is automatically satisfied since we take a P_1 approximation for v_0 and the Eq. (3.9) is solved by a spectral method on the space of ϵ-periodic functions with sufficiently large degrees of freedom.

Remark 3.1.
- *By* (2.4) v_1 *in* (3.9) *has a representation* $v_1(x,y) = \epsilon\chi(y)\nabla u_0(x) + \epsilon\theta(x,y) + r(x,y)$ *on each* ∂K. *The finite element space for approximation of* v_1 *will be designed to best approximate* $\epsilon\chi(y)\nabla u_0(x)$ *in* K, *ignoring the other terms.*
- *To solve* v_1 *in* (3.9) *we can apply the oversampling technique in* [6, 7] *as follows.*

$$\begin{aligned} -\nabla\cdot(a_\epsilon\nabla\gamma) = \nabla\cdot((a_\epsilon-\overline{a})\nabla v_0) &\qquad \textit{in } K', \\ \gamma = 0 &\qquad \textit{on } \partial K', \end{aligned} \tag{3.10}$$

with the oversampling domain K' *of* K. *Then* $v_1 = \gamma|_K - c$ *with* $c = \frac{1}{|\partial K|}\int_{\partial K}\gamma ds$.

Instead of solving the Eq. (3.6) we even substitute g_f with a coarse scale solution g_0 satisfying

$$-\nabla\cdot(\overline{a}\nabla g_0) = \overline{f} \text{ in } K, \qquad \int_e g_0 ds = 0 \text{ on } e \subset \partial K,$$

Indeed, it is easy to see that g_0 can be obtained analytically on each K in the following form.

$$g_0(x,y) = -\frac{\overline{f}}{4\overline{a}}(x^2+y^2) + (c_0 + c_1 x + c_2 y).$$

Using the theory of interpolation, we can easily obtain the following estimates for g_0 whose proof is omitted here.

Lemma 3.2. *It holds*

$$\begin{aligned} \|\nabla g_0\|_{0,K} &\lesssim h\|f\|_{0,K}, \\ \|g_0\|_{0,K} &\lesssim h^2\|f\|_{0,K}. \end{aligned}$$

Then, instead of (3.4) we consider the approximate formula for u_ϵ and its flux as follows:

$$\begin{aligned} \nabla u_\epsilon &\approx \nabla v_\epsilon^h, \\ a_\epsilon\nabla u_\epsilon &\approx a_\epsilon\nabla v_\epsilon^h + \overline{a}\nabla g_0. \end{aligned} \tag{3.11}$$

4. A MULTISCALE FINITE ELEMENT METHOD

In this section we introduce a locally conservative method and its numerical analysis.

Let $V_h \subset H_0^1(\Omega)$ be the space of the conforming P_1 elements for a triangulation $\mathcal{T}_h$, which is the finite element space for v_0 and let

$$Q_h := \{\psi : \epsilon\text{-periodic}, \quad \int_{[0,\epsilon]\times[0,\epsilon]} \psi dx = 0\}$$

be the function space for approximation of v_1. We assume that the dimension of Q_h is taken as large as we want so that χ in (2.3) will be found almost exactly within Q_h. In view of (3.7), set

$$v_\epsilon^h = v_0^h + v_1^h, \quad v_0^h \in V_h,\ v_1^h \in Q_h.$$

Then, $v_0^h \in V_h$ satisfies the Eq. (3.8) automatically. Using that ∇v_0^h is a constant vector, the Eq. (3.9) is reduced to find $\chi \in Q_h$ such that

$$(a_\epsilon \nabla\chi, \nabla\mu)_{Y_\epsilon} = \frac{1}{\epsilon}(\nabla \cdot a_\epsilon, \mu)_{Y_\epsilon}, \quad \mu \in Q_h \tag{4.1}$$

for $Y_\epsilon = [0,\epsilon]\times[0,\epsilon]$, and

$$v_1^h = \epsilon\chi\nabla v_0^h.$$

Note that the Eq. (4.1) is an ϵ-scaled version of (2.3). Then,

$$v_\epsilon^h = v_0^h + \epsilon\chi\nabla v_0^h \tag{4.2}$$

and it satisfies

$$\nabla\cdot(a_\epsilon\nabla v_\epsilon^h) = \nabla\cdot(a_\epsilon(I+\epsilon\nabla\chi)\nabla v_0) = 0. \tag{4.3}$$

Let us introduce the multiscale element space:

$$V_\epsilon^h = \{v_\epsilon : v_\epsilon = v_0 + \epsilon\chi\nabla v_0,\ \ v_0 \in V_h\}.$$

A construction of homogenization-based finite element basis is also considered in [29, 1].

In view of the flux formula (3.11), we consider an approximate flux representation:

$$a_\epsilon\nabla u_\epsilon^h = a_\epsilon\nabla v_\epsilon^h + \overline{a}\nabla g_0.$$

Then our hybrid multiscale finite element method is to find $v_\epsilon^h \in V_\epsilon^h$ (equivalently, find $v_0 \in V_h$) such that

$$\int_{\mathcal{K}_h} [[a_\epsilon\nabla v_\epsilon^h]] w ds = -\int_{\mathcal{K}_h} [[\overline{a}\,\nabla g_0]] w ds \quad \text{for } w \in V_h. \tag{4.4}$$

Implementation of (4.4) is done as follows:

: Step1: Let

$$v_0^h = \sum_{j=1}^{N} c_j \phi^j(x) \in V_h,$$

where $\{\phi^j\}$ is a basis for V_h.

: Step2: Construct multiscale basis $\phi_\epsilon^j = \phi^j + \epsilon\chi\nabla\phi^j$ as in (4.2). Then

$$v_\epsilon^h = \sum_{j=1}^{N} c_j \phi_\epsilon^j \in V_\epsilon^h.$$

: Step3: Solve for $\{c_j\}_{j=1}^N$ the linear system,

$$\sum_{j=1}^{N} c_j \int_{\mathcal{K}_h} [[a_\epsilon \nabla \phi_\epsilon^j]]\phi^i ds = -\int_{\mathcal{K}_h} [[\overline{a}\ \nabla g_0]]\phi^i ds, \quad i = 1:N.$$

Therefore, it is a square system and ellipticity and convergence analysis follow.
By using the Eq. (4.3) and the integration by parts, the left hand side of (4.4) satisfies

$$\begin{aligned}
\int_{\mathcal{K}_h} [[a_\epsilon \nabla v_\epsilon^h]] w ds &= \sum_{K\in\mathcal{T}_h} \langle (a_\epsilon \nabla v_\epsilon^h)\cdot\nu, w\rangle_{\partial K}, \quad w \in V_h \\
&= (a_\epsilon \nabla v_\epsilon^h, \nabla w)_h \\
&= (a_\epsilon(I+\epsilon\nabla\chi)\nabla v_0^h, \nabla w)_h \\
&= (a_0 \nabla v_0^h, \nabla w).
\end{aligned}$$

Using $\int_e g_0 ds = 0$ on $e \subset \partial K$ and $\nabla\cdot(\overline{a}\nabla w) = 0$ on K for $w \in V_h$, we have

$$(\overline{a}\nabla g_0, \nabla w)_K = -(g_0, \nabla\cdot(\overline{a}\nabla w))_K + \langle g_0, (\overline{a}\nabla w)\cdot\nu\rangle_{\partial K} = 0.$$

Therefore, the right hand side of (4.4) satisfies

$$\begin{aligned}
\int_{\mathcal{K}_h} [[\overline{a}\nabla g_0]] w ds &= (\nabla\cdot(\overline{a}\nabla g_0), w)_\Omega + (\overline{a}\nabla g_0, \nabla w)_h, \quad w \in V_h \\
&= -(\overline{f}, w)_\Omega.
\end{aligned}$$

The LC-MsFE method (4.4) can be rewritten in the following variational form: Find $v_0^h \in V^h$ such that

$$(a_0 \nabla v_0^h, \nabla w)_h = (\overline{f}, w)_\Omega, \quad w \in V_h, \tag{4.5}$$

which corresponds to a finite element method for a homogenized Eq. (2.2). The following error estimate is a standard, well-known result in the theory of finite elements.

Theorem 4.1. *Suppose $u_0 \in H^2(\Omega)$ be the solution of the homogenized Eq.* (2.2) *and v_0^h be the solution of* (4.5)*. Then,*

$$\begin{aligned}
\|\nabla(u_0 - v_0^h)\|_{0,\Omega} &\lesssim h\|f\|_{0,\Omega}, \\
\|u_0 - v_0^h\|_{0,\Omega} &\lesssim h^2\|f\|_{1,\Omega}.
\end{aligned}$$

Proof. It is easy to see that

$$(a_0\nabla v_0^h, \nabla w)_h = (a_0\nabla u_0, \nabla w)_h + (\overline{f} - f, w)_\Omega.$$

Simple calculation yields that

$$(a_0\nabla(v_0^h-\psi),\nabla w)_h=(a_0\nabla(u_0-\psi),\nabla w)_h-(f,w-\overline{w})_\Omega,\quad \psi\in V_h.$$

Then, the energy norm estimate follows immediately by choosing ψ suitably and by an elliptic regularity estimate $\|u_0\|_{2,\Omega}\lesssim\|f\|_{0,\Omega}$

Next, for the L_2 estimate, employ a duality argument. Let $e_h=u_0-v_0^h$ and consider w such that $-\nabla\cdot(a_0\nabla w)=e_h$ on Ω and $w=0$ on $\partial\Omega$. Then,

$$\begin{aligned}(e_h,e_h)_\Omega &= (a_0\nabla e_h,\nabla w)_\Omega\\ &= (a_0\nabla e_h,\nabla(w-\psi))_\Omega+(a_0\nabla e_h,\nabla\psi)_\Omega,\quad \psi\in V_h\\ &= (a_0\nabla e_h,\nabla(w-\psi))_\Omega+(f-\overline{f},w)_\Omega\\ &= (a_0\nabla e_h,\nabla(w-\psi))_\Omega+(f-\overline{f},w-\overline{w})_\Omega\end{aligned}$$

By choosing an optimal ψ, we have

$$\|e_h\|_{0,\Omega}^2\lesssim(h\|\nabla e_h\|_{0,\Omega}+h^2\|f\|_{1,\Omega})\|w\|_{2,\Omega}.$$

With an elliptic regularity estimate $\|w\|_{2,\Omega}\lesssim\|e_h\|_{0,\Omega}$ we obtain

$$\|e_h\|_{0,\Omega}\lesssim(h\|\nabla e_h\|_{0,\Omega}+h^2\|f\|_{1,\Omega}).$$

The desired L_2 estimate follows from the help of the energy norm estimate. □

Let us introduce a multiscale interpolation: for $u_\epsilon=u_0+\epsilon\chi\nabla u_0+\epsilon\theta+r$ (see (2.4)), define

$$I_hu_\epsilon=u_{0,I}+\epsilon\chi\nabla u_{0,I}\in V_\epsilon^h,$$

where $u_{0,I}\in V_h$ is the standard P_1 interpolation of u_0 in V_h.

Theorem 4.2. *For $u_\epsilon=u_0+\epsilon\chi\cdot\nabla u_0+\epsilon\theta+r$ with $u_0\in H^2(\Omega)\cap W_\infty^1(\Omega)$, the multiscale interpolation I_h has the following error estimates.*

$$\|u_\epsilon-I_hu_\epsilon\|_j\lesssim\begin{cases}(h^2+\epsilon)\|u_0\|_{2,\Omega}, & j=0,\\ (h+\sqrt{\epsilon})(\|u_0\|_{2,\Omega}+\|u_0\|_{1,\infty,\Omega}), & j=1.\end{cases}$$

Proof. Note that

$$u_\epsilon-I_hu_\epsilon=(u_0-u_{0,I})+\epsilon\chi\nabla(u_0-u_{0,I})+\epsilon\theta+r.$$

Hence, using the standard error estimate of $(u_0-u_{0,I})$ and the estimate (2.6),

$$\begin{aligned}\|u_\epsilon-I_hu_\epsilon\|_{0,\Omega} &\lesssim \|u_0-u_{0,I}\|_{0,\Omega}+\epsilon\|\nabla(u_0-u_{0,I})\|_{0,\Omega}+\|\epsilon\theta+r\|_{0,\Omega}\\ &\lesssim (h^2+\epsilon h+\epsilon)\|u_0\|_{2,\Omega}\end{aligned}$$

Note that

$$\nabla(u_\epsilon-I_hu_\epsilon)=\nabla(u_0-u_{0,I})+\epsilon(\nabla\chi)\nabla(u_0-u_{0,I})+\epsilon\chi\Delta u_0+\epsilon\nabla\theta+\nabla r.$$

The estimates (2.5) yield

$$\|\nabla(u_\epsilon-I_hu_\epsilon)\|_{0,\Omega}\lesssim(h+\epsilon+\sqrt{\epsilon})(\|u_0\|_{2,\Omega}+\|u_0\|_{1,\infty,\Omega}).$$

□

Theorem 4.3. *Let $v_\epsilon=v_0^h+\epsilon\chi\nabla v_0^h\in V_\epsilon^h$ be the solution of* (4.4) *and u_ϵ be the exact solution of* (1.1) *with $u_0\in H^2(\Omega)\cap W_\infty^1(\Omega)$. Then,*

$$\|u_\epsilon-v_\epsilon\|_{j,h}\lesssim\begin{cases}(h^2+\epsilon)\|f\|_{0,\Omega}, & j=0,\\ (h+\sqrt{\epsilon})(\|f\|_{0,\Omega}+\|u_0\|_{1,\infty,\Omega}), & j=1.\end{cases}$$

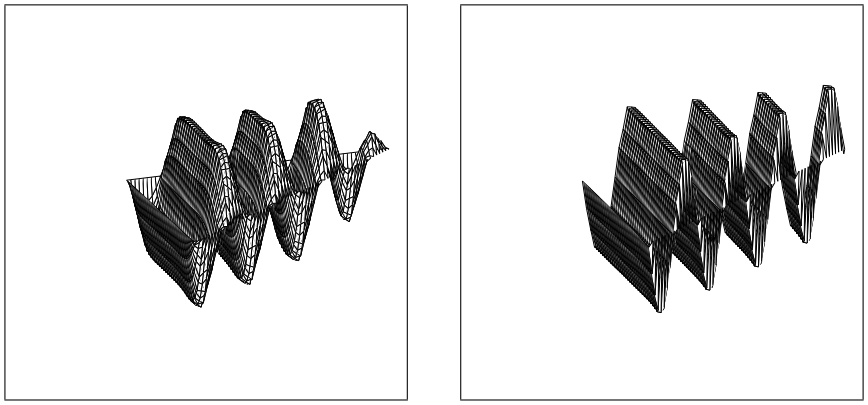

Figure 1: The solutions of the Eq. (3.10) without the oversampling (left) and with the oversampling (right).

Proof. Simple calculation yields that

$$\begin{aligned} v_\epsilon - I_h u_\epsilon &= (v_0^h - u_{0,I}) + \epsilon\chi\nabla(v_0^h - u_{0,I}), \\ \nabla(v_\epsilon - I_h u_\epsilon) &= \nabla(v_0^h - u_{0,I}) + \epsilon(\nabla\chi)\cdot\nabla(v_0^h - u_{0,I}). \end{aligned}$$

Using the estimates in Theorem 4.1,

$$\begin{aligned} \|v_\epsilon - I_h u_\epsilon\|_{0,\Omega} &\lesssim (h^2 + \epsilon h)\|f\|_{0,\Omega}, \\ \|v_\epsilon - I_h u_\epsilon\|_{0,\Omega} &\lesssim h\|f\|_{0,\Omega}. \end{aligned}$$

The triangle inequality with estimates in Theorem 4.2 yields the desired estimate. □

5. NUMERICAL EXPERIMENTS

In this section we concentrate on numerical experiments for the LC-MsFE method. We consider two different ways of the fine scale resolution construction: the spectral approach by solving the Eq.

Table 1: The L_2 and H^1 convergence: ϵ-interference.

	$\epsilon = 1/3200$				$\epsilon = 1/64$			
N	L_2	α	H^1	α	L_2	α	H^1	α
8	4.759e-3		1.563e-1		4.761e-3		1.563e-1	
16	1.158e-3	2.04	7.644e-2	1.03	1.271e-3	1.91	7.644e-2	1.03
32	2.858e-4	2.02	3.778e-2	1.02	5.788e-4	1.13	3.778e-2	1.02
64	7.155e-5	2.00	1.878e-2	1.01	5.122e-4	0.18	2.062e-2	0.87

Table 2: The L_2 and H^1 convergence: the h-ϵ resonance with $h = \epsilon$.

N	L_2	α	H^1	α
8	5.928e-3		1.707e-1	
16	2.289e-3	1.37	8.370e-2	1.03
32	1.049e-3	1.13	4.144e-2	1.01
64	5.122e-4	1.03	2.062e-2	1.01

(4.1) in a periodic function space (Tables 1-3) and the oversampling approach by solving (3.10) in a finite element space (Table 4), see Fig. 1.

Example: *We consider the following (quasi-two-dimensional) model problem* [30]*:*

$$\begin{aligned} -\nabla\cdot(a_\epsilon\nabla u_\epsilon) &= f \quad \textit{in } \Omega=(0,1)^2,\\ u_\epsilon|_{\Gamma_D} &= 0 \quad \textit{on } \Gamma_D:=\{x_1=0\}\cup\{x_1=1\},\\ \nu\cdot(a_\epsilon\nabla u_\epsilon)|_{\Gamma_N} &= 0 \quad \textit{on } \Gamma_N:=\partial\Omega\setminus\Gamma_D, \end{aligned}$$

where

$$a(y)=\frac{1}{2+\cos 2\pi y_1},\quad y=(y_1,y_2)\in Y=[0,1]^2,$$

and $f(x)=1$. *The exact solution is known analytically as follows:*

$$u_\epsilon(x_1,x_2)=-x_1^2-\frac{\epsilon}{2\pi}x_1\sin(\frac{2\pi x_1}{\epsilon})-\frac{\epsilon^2}{4\pi^2}(\cos(\frac{2\pi x_1}{\epsilon})-1)+x_1+\frac{\epsilon}{4\pi}\sin(\frac{2\pi x_1}{\epsilon}).$$

The computational domain $\Omega:=(0,1)^2$ is divided into a uniform mesh so that the vertices are given as $x_1^i=ih$ and $x_2^j=jh$, $h=1/N$ for $0\le i,\ j\le N$ and the triangular mesh is then generated by bisecting each rectangle by a diagonal line. The computational meshes are composed of $2N^2$-triangles with $N=8,\ 16,\ 32,\ 64$. The local resolution χ in (4.1) is solved in the space of ϵ-periodic functions of degrees up to two for numerical results in Tables 1-3.

Through numerical tests the following important issues on our numerical scheme are addressed;

: 1. the effect of ϵ-*interference* and ϵ-h *resonance*,

: 2. the effect of *phase shift* when the size of a triangle is not an integer multiple of ϵ.

In Tables 1, 2 and 4, the L_2 and H^1 errors represent

$$L_2:=\|u_\epsilon-v_\epsilon^h\|_{0,\Omega}\quad\text{and}\quad H^1:=\|\nabla u_\epsilon-\nabla v_\epsilon^h\|_{0,h},$$

and α denotes convergence orders.

The cost of computation is mostly involved in solving the coarse system and it does not depend on the size of ϵ.

Table 3: The L_2 and H^1 convergence of the effective solution: phase-shift interference.

	$\epsilon=1/1019$				$\epsilon=1/121$			
N	L_2	α	H^1	α	L_2	α	H^1	α
8	4.755e-3		5.413e-2		5.681e-3		5.467e-2	
16	1.159e-3	2.04	2.708e-2	1.00	1.363e-3	2.06	2.917e-2	0.91
32	2.873e-4	2.01	1.357e-2	1.00	4.304e-4	1.66	1.782e-2	0.71
64	7.821e-5	1.88	6.840e-3	0.99	2.858e-4	0.59	1.358e-2	0.39

Table 4: The L_2 and H^1 convergence of the oversampling local solver

	$\epsilon=1/128$				$\epsilon=1/256$			
N	L_2	α	H^1	α	L_2	α	H^1	α
8	1.232 e-2		1.030 e-1		4.76 6e-2		2.044 e-1	
16	3.491 e-3	1.82	4.801 e-2	1.10	1.037 e-2	2.20	6.354 e-2	1.69
32	1.182 e-3	1.56	2.359 e-2	1.03	2.985 e-3	1.80	2.564 e-2	1.31
64	6.236 e-4	0.92	4.207 e-3	2.49	1.055 e-3	1.50	1.203 e-2	1.09

Tables 1 & 2 address the effect of ϵ-interference. According to numerical analysis we expect the following convergence:

$$\|u_\epsilon - v_\epsilon^h\|_{0,\Omega} = O(h^2 + \epsilon), \quad \|u_\epsilon - v_\epsilon^h\|_{1,h} = O(h + \sqrt{\epsilon}). \tag{5.1}$$

Therefore, there can be interference of ϵ when the mesh size h gets close to $\sqrt{\epsilon}$. As expected, Table 1 shows that there is no interference of ϵ when $0 < \epsilon << h$ and there begins to appear ϵ-interference when $\epsilon \approx h$. The ϵ interference must be distinguished from the *so called* ϵ-h resonance in [7, 8]. The ϵ-h resonance means that approximate solutions may not converge when the ratio, ϵ/h is kept constant. Table 2 shows that our method is independent from the ϵ-h resonance. We may expect the rates of convergence:

$$\|u_\epsilon - v_\epsilon^h\|_{0,\Omega} = O(h), \quad \|u_\epsilon - v_\epsilon^h\|_{1,h} = O(\sqrt{h})$$

for $\epsilon = h$ from (5.1). The L_2-error shows the expected rate of convergence, however the H^1-error performs better than the above expectation.

Table 3 shows the effect of phase shift in numerical solutions. If h is not an integer multiple of ϵ, there can be different shift for each triangle in the periodic part (local fine resolution) of solutions according to the location of a triangle K in the domain Ω. Our numerical scheme ignores these shifts to avoid algorithmic complication. Therefore, the fine scale error $(u_\epsilon - v_\epsilon^h)$ must contain a lot of shift errors. However, the effect of phase shift can be ignored if one looks at coarse scale errors. In Table 3 coarse scale errors are measured in the coarse L_2 and H^1-norms, that is,

$$L_2 = \|P_h(u_\epsilon - v_\epsilon^h)\|_{0,\Omega} \quad \text{and} \quad H^1 = \|\overline{\nabla u_\epsilon} - \overline{\nabla v_\epsilon^h}\|_{0,h},$$

where $P_h(u_\epsilon) \in X_h$ represents the usual piecewise P_1 interpolation and $\overline{u_\epsilon}$ represents the cell average of u_ϵ for each K. It shows a regular convergence behavior in a coarse scale when ϵ/h is small. As ϵ/h approaches 1, convergence deteriorates. Compared with Table 2, the irregular convergence behavior seems to be mainly due to the ϵ-interference.

When the conductivity coefficient a_ϵ is non-periodic the oversampling technique introduce by Hou and Wu [7] is inevitable. Therefore, we introduce the LC-MsFE combined the oversampling method and provide related numerical results in Table 4. In this case the Eq. (3.10) is solved for γ by a numerical method and we use the non-conforming cell boundary element method [19] since the accurate flux information is important.

In conclusion, computational cost is mainly involved in solving the coarse scale problem with the spectral local solver. With the oversampling approach the local basis construction can be very expensive when ϵ is very small and the most of the computing time can be taken for this process. Therefore, the oversampling approach may not be feasible for an extremely small ϵ, however, it can be applied to the problems with a more general type of conductivity. Our method has a power of resolving fine scale resolutions when the mesh size is an integer multiple of ϵ. When the mesh size is not an integer multiple of ϵ, a postprocessing with proper phase shift will reproduce fine scale resolution on cells wanted. We close this section with a remark that one can apply the adaptive variational multiscale method [31] which makes use of multiscale-type a posteriori error estimators to adapt the coarse and fine scale meshsizes as well as the fine-problem patch-sizes.

ACKNOWLEDGMENT

Y. JEON was supported by National Research Foundation of Korea grant funded by the Korea government (2018R1D1A1A09082082). E.-J. PARK was supported by National Research Foundation of Korea grant funded by the Korea government (NRF-2015R1A5A1009350).

REFERENCES

[1] T. Arbogast, Homogenization-based mixed multiscale finite elements for problems with anisotropy, Multiscale Modeling and Simulation 9 (2) (2011), pp. 624-653.

[2] A. Bensoussan, J.-L. Lions, G. Papanicolaou, Asymptotic Analysis for periodic Structures, North-Holland, Amsterdam, 1978.

[3] T. J. R. Hughes, G. R. Feijoo, L. Mazzei, J.-B. Quincy, The variational multiscale method. A paradigm for computational mechanics, Comput. Methods Appl. Mech. Engrg. 166 (1998) 3-24.

[4] J. T. Oden, K. S. Vemaganti, Adaptive hierarchical modeling of heterogeneous structures, Phys. D 133 (1999) 404-415.

[5] Z. Chen, T. Y. Hou, A mixed multiscale finite element method for elliptic problems with oscillating coefficients, Math. Comp. 72 (2003) 541-576.

[6] Y. Efendiev, T. Hou, Multiscale Finite Element Methods, Theory and Applications, Surveys and Tutorials in the Applied Mathematical Sciences, vol.4. Springer, New York, 2009.

[7] T. Y. Hou, X.-H. Wu, A multiscale finite element method for elliptic problems in composite materials and porous media, J. Comput. Phys. 134 (1997) 169-189.

[8] T. Y. Hou, X.-H. Wu, Y. Zhang, Removing the cell resonance error in the multiscale finite element method via a Petrov-Galerkin formulation, Commun. Math. Sci. 2 (2) (2004) 185-205.

[9] F. Brezzi, Interacting with the subgrid world, in: Numerical Analysis 1999 (Dundee), in: Chapman & Hall/CRC Res. Notes Math., vol. 420, Chapman & Hall/CRC, Boca Raton, FL, 2000, pp. 69-82.

[10] G. Sangalli, Capturing small scales in elliptic problems using a residual-free bubbles finite element method, Multiscale Model. Simul. 1 (2003) 485-503.

[11] W. E, B. Engquist, The heterogeneous multi-scale methods, Commun. Math. Sci. 1 (1) (2003) 87-132.

[12] R. Du, P. Ming, Convergence of the heterogeneous multiscale finite element method for ellitpic problems with nonsmoothe microstructures, Multisclae Model. Simul. 8(5) (2010) 1770-1783.

[13] C. Schwab, A.-M. Matache, Generalized FEM for homogenization problems, in: Multiscale and Multiresolution Methods, in: Lect. Notes Comput. Sci. Eng., vol. 20, Springer-Verlag, Berlin, 2002, pp. 197-237.

[14] T. Arbogast, G. Pencheva, M. F. Wheeler, and I. Yotov, A multiscale mortar mixed finite element method. Multiscale Model. Simul. Vol. 6, No. 1, (2007), pp. 319–346.

[15] M.-Y. KIM, E.-J. PARK, S. G. THOMAS, AND M. F. WHEELER, A multiscale mortar mixed finite element method for slightly compressible flows in porous media, *J. Korean Math. Soc.* 44 (2007), No. 5, pp. 1103-1119

[16] M. Arshad, E.-J. Park, and D.-w. Shin, Analysis of Multiscale Mortar Mixed Approximation of Nonlinear Elliptic Equations, Computers & Mathematics with Applications, Vol 75, No. 2, (2018), 401-418

[17] M.-Y. KIM AND M. F. WHEELER, *A multiscale discontinuous galerkin method for convection–diffusion–reaction problems*, Computers & Mathematics with Applications, 68 (2014), pp. 2251–2261.

[18] Y. Jeon, A multiscale cell boundary element method for elliptic problems, Appl. Numer. Math. 59 (11) (2009) 2801-2813.

[19] Y. Jeon, E.-J. Park, Nonconforming cell boundary element methods for elliptic problems on triangular mesh, Appl. Numer. Math. 58 (6) (2008) 800–814.

[20] Y. Jeon, E.-J. Park, A hybrid discontinuous Galerkin method for elliptic problems, SIAM J. Numer. Anal. 48 (5) (2010) 1968-1983.

[21] Y. Jeon, E.-J. Park, New locally conservative finite element methods on a rectangular mesh, Numerische Mathematik, 123 (2013), no.1, 97-119.

[22] Y. Jeon, and E.-J. Park, D.-w. Shin, Hybrid Spectral Difference Methods for an Elliptic Equation, Comput. Methods Appl. Math. vol.17 no.2 (2017), 253-267.

[23] M.-Y. KIM AND M. F. WHEELER, *Coupling discontinuous Galerkin discretizations using mortar finite elements for advection–diffusion–reaction problems*, Computers & Mathematics with Applications, 67 (2014), pp. 181–198.

[24] Y. Jeon, E.-J. Park, D. Sheen, A hybridized finite element method for the Stokes problem, Computers & Mathematics with Applications Vol. 68, No. 12 Part B, (2014), 2222-2232.

[25] D.-w. Shin, Y. Jeon, and E.-J. Park, A hybrid discontinuous Galerkin method for advection-diffusion-reaction problems, Applied Numerical Mathematics, 95 (2015), 292-303.

[26] L. Zhao and E.-J. Park. A new hybrid staggered discontinuous Galerkin method on general meshes. *Journal of Scientific Computing*, 82:12, 2020.

[27] P. Jenny, S. H. Lee, H. A. Tchelepi, Multi-scale finite-volume method for elliptic problems in subsurface flow simulation, J. Comput. Phys. 187 (2003) 47-67.

[28] V. V. Jikov, S. M. Kozlov, O. A. Oleinik, Homogenization of Differential Operators and Integral Functionals, Springer-Verlag, Berlin, Heidelberg, 1994.

[29] G. Allaire, R. Brizzi, A multiscale finite element method for numerical homogenization, Multiscale Model. Simul. 4 (3) (2005) 790-812.
[30] A. Abdulle, W. E, Finite difference HMM for homogenization problems, J. Comput. Phys. 191 (2003) 18-39.
[31] M. G. Larson and A. Målqvist, Adaptive variational multiscale methods based on a posteriori error estimation: Energy norm estimates for elliptic problems, Computer Methods in Applied Mechanics and Engineering 196 (2007), no. 21-24, 2313-2324.